PRESCIENT: A predictive channel access scheme for IEEE 802.15.4-compliant devices considering IEEE 802.11 coexistence

Tolga ÇÖPLÜ*, **Sema Fatma OKTUĞ**
Department of Computer Engineering, İstanbul Technical University, İstanbul, Turkey

Abstract: Coexistence is among the most significant challenges for IEEE 802.15.4-compliant devices in indoor environments. Previous works have shown that IEEE 802.11-compliant devices are the major sources of interference in the 2.4 GHz industrial, scientific, and medical band. In order to overcome the coexistence problem, IEEE 802.15.4-compliant devices should monitor the communication channel and access the channel when it is not in use. In this study, the impact of IEEE 802.11 traffic on IEEE 802.15.4 communication is analyzed and a novel predictive channel access scheme, PRESCIENT (PREdictive channel access SCheme for IEee 802.15.4-compliaNT devices), is proposed. The performance evaluation of the proposed scheme is performed using real-world radio frequency signal strength measurements. The results show that the proposed scheme achieves significant performance improvement in terms of channel access under IEEE 802.11 interference.

Key words: Coexistence, IEEE 802.15.4, predictive channel access, IEEE 802.11

1. Introduction

Technological advancements in wireless communications lead to increasing indoor applications at the consumer end. Consumer devices that adjust ambient temperature and room lighting based on the occupancy of the home are just a few to name. These and similar devices help to increase the quality of human life as well as contribute to energy savings. With these motivations, many IEEE 802.15.4-compliant [1] devices that communicate over the 2.4 GHz industrial, scientific, and medical (ISM) band have been developed. However, the 2.4 GHz ISM band is not specifically assigned to the devices employing the IEEE 802.15.4 standard; it is also utilized by other devices employing standards such as IEEE 802.11 [2] and IEEE 802.15.1 [3]. Those standards are widely adopted by consumer devices for indoor environments and they cause interference for the IEEE 802.15.4-compliant devices. In addition, microwave ovens can cause interference in the same ISM band [4–6]. Interference issues can be very severe with the increasing number of devices operating in the 2.4 GHz ISM band since 2.4 GHz is the only global ISM band. Therefore, coexistence arises as a big challenge especially for the IEEE 802.15.4-compliant devices because of their relatively low transmission power, data rate, and buffer capacity.

Studies on the coexistence of IEEE 802.15.4-compliant devices have mainly focused on the IEEE 802.11-related interference [6–11]. IEEE 802.11 devices have approximately 30 to 100 times higher transmission power than that of IEEE 802.15.4-compliant devices. As a result, the coexistence of IEEE 802.11 and IEEE 802.15.4 devices has asymmetric interference patterns, as stated in [9,11]. The IEEE 802.15.4 standard provides several mechanisms to handle the coexistence problem, such as the modulation technique, low duty cycling,

---

*Correspondence: coplu@itu.edu.tr

low transmit power, dynamic channel selection, and clear channel assessment (CCA) with energy detection (hereafter referred to as simply CCA) [12]. However, performance evaluations show that these techniques are still far from eliminating the negative effects of IEEE 802.11 devices on the communication performance of IEEE 802.15.4-compliant devices. Consequently, the performance of IEEE 802.15.4-compliant devices under IEEE 802.11 interference is far from tolerable and needs further research.

In the literature, there are studies from various perspectives about the coexistence of IEEE 802.11 and IEEE 802.15.4-compliant devices. Nearly 70 papers on the coexistence of IEEE 802.11 and IEEE 802.15.4 technologies were systematically analyzed in [13] by covering future research developments and open research issues. In [14], a novel short response time recovery scheme was proposed to enhance the coexistence performance of the beacon-enabled IEEE 802.15.4 networks under IEEE 802.11 interference. Also, an adaptive interference-aware multichannel clustering algorithm was proposed for the IEEE 802.15.4 cluster-tree networks [15]. An energy-efficient distributed channel selection scheme was proposed for dynamic IEEE 802.11 interference [9]. In [16], a simple adaptive interference avoidance scheme using a dynamic channel selection method based on the variance of received signal strength indicator (RSSI) was proposed. In general, all these proposed methods focused on adaptive or dynamic channel selection schemes to improve the coexistence performance of IEEE 802.15.4-compliant devices. It has been observed that switching to an idle (or seldom active) channel improves the communication performance of IEEE 802.15.4-compliant devices significantly. Therefore, adaptive or dynamic channel selection schemes have been among the most popular methods to improve interchannel coexistence. However, the proposed methods are not capable of avoiding innerchannel interference. Given the rapid increase in the number of devices communicating in the 2.4 GHz ISM band, it is clear that innerchannel interference needs to be addressed to improve the coexistence performance. In our previous work [17], we proposed a scheme to address the innerchannel interference problem, which used clustering techniques to enhance the free channel access performance of IEEE 802.15.4-compliant devices. In that work, we showed that the proposed scheme can provide significant coexistence performance improvement.

In this study, in order to achieve better coexistence performance of the IEEE 802.15.4-compliant devices, we introduce a novel inner channel access scheme called PRESCIENT (PREdictive channel access SCheme for IEee 802.15.4-compliaNT devices). Our main goal is to boost the free channel access performance, thus preventing ineffective use of the channel bandwidth caused by packet retransmissions. To the best of our knowledge, PRESCIENT is the first innerchannel prediction scheme in the literature that can be embedded in IEEE 802.15.4-compliant devices.

This paper is organized as follows: Section 2 presents the impacts of aggregated IEEE 802.11 traffic on the channel access performance of IEEE 802.15.4-compliant devices. In Section 3, the proposed scheme, PRESCIENT, is explained in detail. Section 4 provides the performance evaluation of the proposed scheme using an IEEE 802.15.4-compliant test bed. Finally, Section 5 concludes the paper by proposing future directions.

2. Impacts of aggregated IEEE 802.11 traffic on IEEE 802.15.4 communications

It is well known that IEEE 802.11 devices are the major interferers in the 2.4 GHz ISM band [6–11,13]. In this work, to analyze the impact of aggregated IEEE 802.11 traffic on the IEEE 802.15.4-compliant wireless sensor network (WSN) nodes, a test bed was designed. The analytical model of IEEE 802.15.4 can be found in [18]. In our work, the radio frequency signal strength (RFSS) measurements of the communication channel, which is the main factor for both CCA and RSSI values, were recorded by using the 2.4 GHz IEEE 802.15.4-compliant products in different RF channels. In our test scenario, 2 pairs of IEEE 802.15.4-compliant products, Pair 1

and Pair 2, are used. In each pair, one node is configured as a transmitter and the other one is configured as a receiver. The nodes with the same functionality are positioned parallel to each other at 25 cm in distance. In this setup, the transmitter nodes measure 2 consecutive CCA values and then transmit these measurements to the corresponding receiver with a unique packet ID. These transmissions are done periodically at an interval of 10 ms. The transmitter nodes log the same packet on a computer via serial wired communication. If the packet is received seamlessly, the receiver node inserts the calculated RSSI value to the packet and sends the packet to a computer via serial wired communication. Note that packet loss rate can be obtained by comparing the packet ID logs of the transmitter and the receiver nodes. The measurements were done for 2 different scenarios: with an IEEE 802.11-idle (no IEEE 802.11 interference) communication channel and with an IEEE 802.11-busy communication channel, respectively. A schematic representation of the test bed is given in Figure 1.
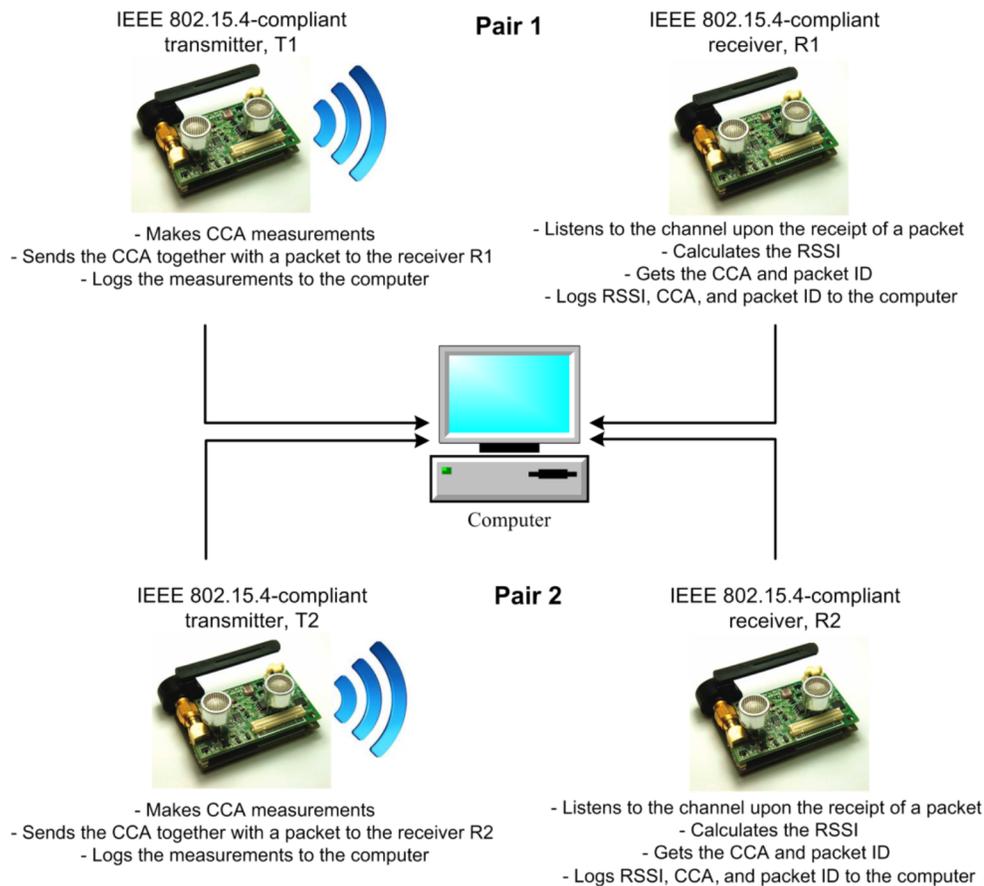

Figure 1. A schematic representation of the test bed.

In the first scenario, called the IEEE 802.11-idle scenario, the RFSS traces (in dBm) were taken in an indoor office environment. A spectrum analyzer was used to confirm that there was no coexistence in the channel. The logged CCA and RSSI measurements are presented in Figure 2. The results show that when the channel is IEEE 802.11-idle, the mean of CCA measurements is about –88 dBm and the variance is about 3.5 dBm for both pairs. Since the means of RSSI measurements are –58 dBm and –59 dBm for Pair 1 and Pair 2, the calculated signal to interference (SIR) values are approximately 30 dBm and 29 dBm, respectively. For such SIR values, packet loss is not anticipated except for some particular environments. As expected, we do not observe any packet loss in the first scenario for both pairs.

In the second scenario, called the IEEE 802.11-busy scenario, the same test bed is used as in the IEEE 802.11-idle scenario. However, this time the IEEE 802.11 devices and access points around the laboratory are enabled. In this environment, neither the number of IEEE 802.11 devices nor the traffic pattern generated by them was manipulated. The traffic of the IEEE 802.11 devices was a result of daily user activities in the offices around. Here our goal is to examine the impact of real-world aggregated background IEEE 802.11 traffic on the IEEE 802.15.4-compliant WSN nodes.

The CCA and RSSI measurements of the WSN nodes are shown in Figure 3. In these tests, we have observed the following:
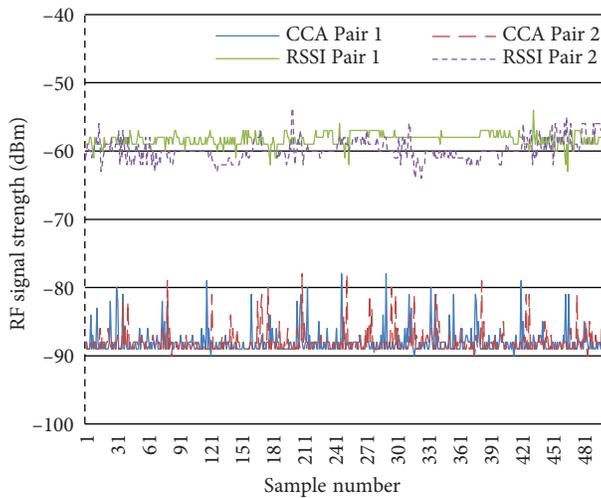

Figure 2. A 500-sample snapshot of CCA and RSSI measurements for the IEEE 802.11-idle scenario.
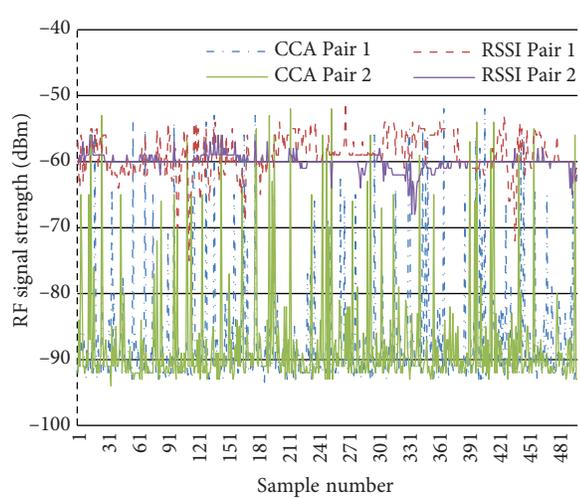
Figure 3. A 500-sample snapshot of CCA and RSSI measurements for the IEEE 802.11-busy scenario.

- The CCA measurements of both transmitter nodes have high variance, as seen in Figure 3, which is due to the presence of IEEE 802.11 traffic.

- Variations in the CCA values for different samples observed in the measurements is reasonable, since there are multiple access points and multiple PCs connected to those access points.

- When measurements are repeated after terminating all the IEEE 802.11 communications in the environment, the fluctuations in the measurements fade away for both pairs.

- CCA and RSSI measurements of Pair 1 and Pair 2 are almost equal, justifying that both pairs observe the same level of interference from IEEE 802.11 traffic.

- A detailed analysis of CCA and RSSI measurements reveals that for Pair 1, in only 7.18% of the observation period there is IEEE 802.11 traffic that forces SIR values to go below 10 dB; however, this causes a packet loss value of 6.92%. For Pair 2, the rate of SIR values lower than 10 dB is 7.06% and the rate of packet loss is 6.88%. Note that a 10 dB threshold is selected because in the literature it is shown that 10 dB is a critical value for the IEEE 802.15.4 standard to provide successful communication [12].

Considering the fact that the communication channel is already IEEE 802.11-idle for 92.82% of the time for Pair 1 and 92.94% for Pair 2, the high packet loss rate of 6.92% for Pair 1 and 6.88% for Pair 2 indicates that the periodic channel access used in the test bed is not efficient enough.

3. PRESCIENT: A predictive channel access scheme for IEEE 802.15.4-compliant devices

Packet loss rate, number of retransmissions, RSSI, CCA, or SIR values, which are commonly used as channel quality features [19,20], cannot be used directly in order to predict the forthcoming channel conditions because these features do not have time relations to predict the instants when the channel is going to be free. Hence, we need other features having time relations to be used in our predictions.

In our studies, we observed that the history of elapsed time between the transmissions of the same interferer can be a convenient feature to represent the channel quality and can help us predict the forthcoming interfered channel instants. Unfortunately, this feature cannot be extracted directly, since proper separation of the interferers is not achievable in practice. Note that the separation of interferers using the CCA measurements is an NP-hard problem and it is not possible to calculate the proposed feature directly on tiny, resource-constrained IEEE 802.15.4-compliant devices. Hence, we assume that close CCA measurements correspond to the same interferer in order to converge to the ideal case in the proposed technique called PRESCIENT. PRESCIENT consists of 3 main modules: the Channel Activity Monitoring Module (CAMM), the Training Module (TM), and the Prediction Module (PM). The CAMM monitors the channel by making CCA measurements and logging them. These logs are delivered to the TM, where transmission history-based prediction coefficients are calculated for each CCA group. In other words, this step is the place where previous transmissions of each interferer are modeled to be used in our predictions. The PM uses the calculated prediction coefficients to assign weights to each forthcoming channel instant. Finally, the channel access decision is made based on the previously calculated instant weights.

3.1. The Channel Activity Monitoring Module (CAMM)

The CAMM, which is implemented in each IEEE 802.15.4-compliant node, monitors the RFSS values of the channel by making CCA measurements at a frequency of f_s. High f_s rates provide more channel activity details but consume more processing capability of the IEEE 802.15.4-compliant device. We set f_s to 100 Hz in our tests. The channel activity vector q is defined as:

$$q = [q(1), q(2), \ldots, q(N)] \in \Re, \tag{1}$$

where N is CAMM sample size.

Once N samples are recorded, the CAMM delivers vector q to TM. Then the CAMM restarts its own process by resetting vector q. During this process, every CCA measurement is compared with an interference threshold λ, which is used for the discrimination between the interference and the interference-free CCA measurements. If the current CCA measurement is higher than λ, then the PM is called. The threshold λ (dBm) is calculated as:

$$\lambda = \mu_{CCA} + \sigma^2_{CCA}, \tag{2}$$

where μ_{CCA} is the mean and σ^2_{CCA} is the variance of the CCA measurements of an IEEE 802.11-idle environment. Note that the value of λ is dependent on both the RF sensitivity of the IEEE 802.15.4-compliant hardware and the background RF noise of the environment. In our test bed, λ is calculated as –80 dBm based on the values obtained in Section 2.

The CAMM works according to the flow diagram given in Figure 4.
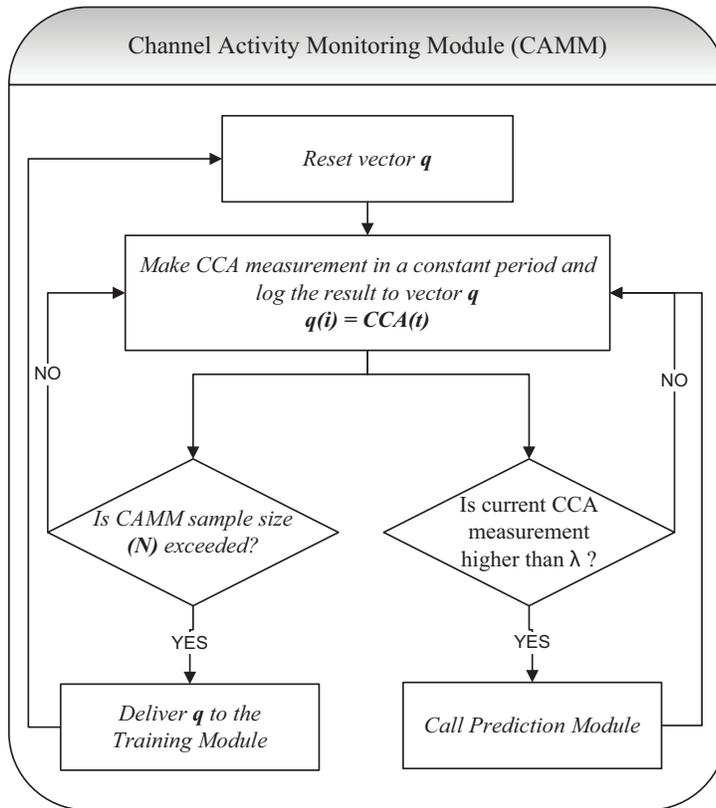
Figure 4. Flow chart of the Channel Activity Monitoring Module (CAMM).

3.2. The Training Module (TM)

The TM is the module where prediction coefficients are calculated. In the first step of the TM process, q values higher than λ are stored in a 2-dimensional vector r, as shown in Figure 5. The first column of r stores the q values while the second column stores the index of the related measurements on q, where K is the number of q values exceeding λ.
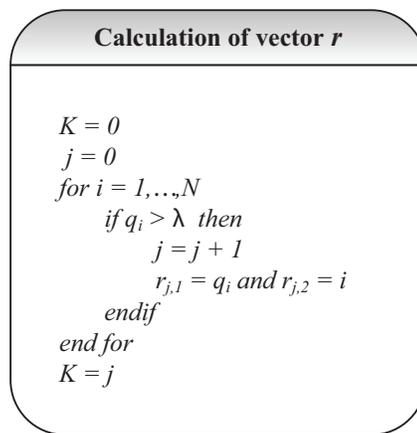

Figure 5. Pseudocode for the calculation of vector r.

In the second step, we calculate the prediction coefficients vector, T_α, by using r. Each prediction coefficient represents the total number of transmissions of an interferer within a certain period. Here we assume that close CCA amplitudes represent the same interferer. According to this assumption, CCA measurements whose differences are smaller than threshold δ are accepted as the same interferer. We propose to use RSSI or CCA accuracy of the RF chip as δ, which is 6 dBm for our test bed devices.

T_α is calculated as follows:

$$T_\alpha(r_{j,2} - r_{i,2}) = \sum_{i=1}^{K-1}\sum_{j=i+1}^{K} 1$$
$$\text{forevery } |r_{j,1} - r_{i,1}| \leq \delta \qquad (3)$$

Now a sample scenario will be given to clarify the calculation of T_α. Let us assume a sequence of CCA measurements as given in Figure 6. Relying on Figure 6, vector q becomes $\{-64,-86,-82,-69,-83,-60,-71\}$ where N is 7. Then, using vector q, the TM calculates vector r as $\{(-64,1), (-69,4), (-60,6), (-71,7)\}$ where K is 4. Finally, T_α becomes $\{0,0,2,0,1,0,0\}$ as given in Eq. (4), where δ is taken as 6.

$$T_\alpha(1) = T_\alpha(2) = T_\alpha(4) = T_\alpha(6) = 0,$$
$$T_\alpha(3) = 1 + 1 = 2 \sin ce\, |(-69) - (-64)| \leq \delta\, and\, |(-71) - (-69)| \leq \delta, \qquad (4)$$
$$T_\alpha(5) = 1 \sin ce\, |(-60) - (-64)| \leq \delta$$
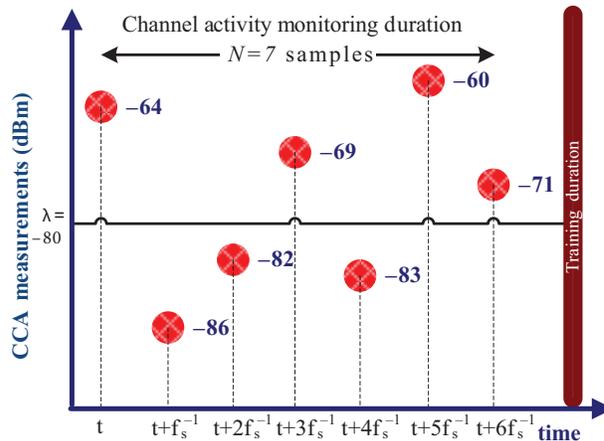

Figure 6. A schematic representation of the CAMM followed by the Training Module.

3.3. The Prediction Module (PM)

The PM uses the T_α vector to update vector W, which holds the weights of the forthcoming channel instants. PM updates vector W according to Eq. (5) when interference is measured by the CAMM.

$$W(i) = W(i) + T_\alpha(i)$$
$$for\, i = 1, ..., L \qquad (5)$$

where L is the prediction window sample size.

The PM clusters the forthcoming channel instants as IEEE 802.11-busy or IEEE 802.11-idle using Eq. (6).

$$\text{ChannelAccess}(n + (ixf_s^{-1})) = \begin{cases} \text{free,} & W(i) < T_{THR} \\ \text{busy,} & \text{otherwise} \end{cases} \qquad (6)$$

where n indicates the current channel instant, f_s is the sampling frequency of the CCA measurements, and T_{THR} is the decision threshold of the proposed scheme. For those entries exceeding T_{THR}, the channel is predicted as busy, and no channel access is scheduled for that instant. As a consequence, T_{THR} has a direct impact on the aggressiveness of the PM, which will be evaluated in the next section.

Figures 7 and 8 illustrate how the proposed scheme works. In these figures, empty bars represent free channel states while dotted bars represent busy channel states. Predicted and measured channel states are given separately. The numbers in the bars represent the related prediction weight values.
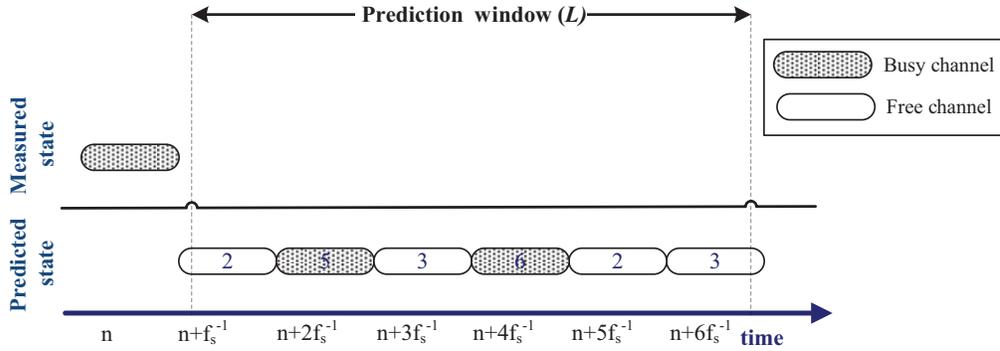

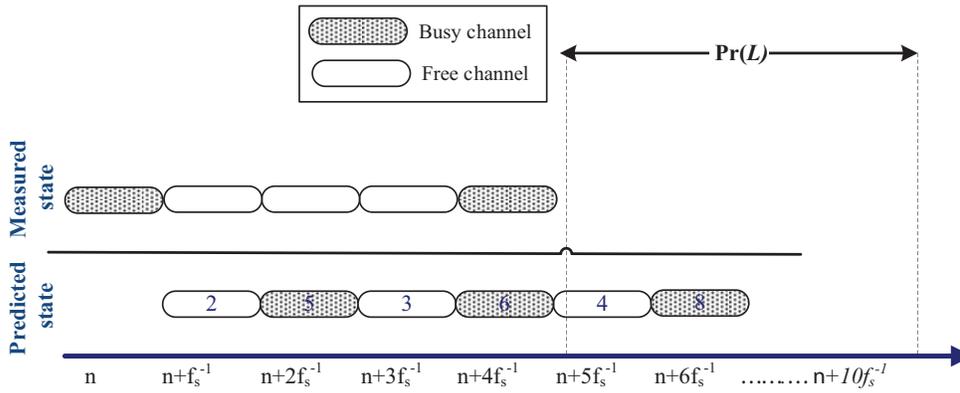**Figure 7.** Predicted channel states at n.

Figure 8. Measured and predicted channel states at $n+4f_s^{-1}$.

Figure 7 shows a sample scenario for PRESCIENT at n, while Figure 8 indicates the status of the same scenario at $n+4f_s^{-1}$. In Figure 7, it is shown that interference is detected at n. According to PRESCIENT, the PM is called by the CAMM right after this instant. When initiated, the PM first calculates the weights of the forthcoming channel instants and then marks them as busy or free based on the threshold value. Figure 8 illustrates the same scenario at $n+4f_s^{-1}$ where interference is detected by CAMM and PM is recalled. Details about this scenario are given below.

- Figure 7 shows that, at n, forthcoming instants are predicted as free for $n + f_s^{-1}$, $n+3f_s^{-1}$, $n+5f_s^{-1}$, $n+6f_s^{-1}$ and busy for $n+2f_s^{-1}$, $n+4f_s^{-1}$.

- According to Figure 8, CAMM measurements comply with the previous predictions for $n+f_s^{-1}$, $n+3f_s^{-1}$, $n+4f_s^{-1}$. However, a false prediction occurred at $n+2f_s^{-1}$. At that instant, a busy channel was predicted but the CAMM measurement showed that the channel was free.

- Figure 8 shows that at $n+4f_s^{-1}$ the CAMM detects interference and the PM is recalled. Therefore, at $n+4f_s^{-1}$ the prediction window is reinitiated. First the weight values for the instants $n+5f_s^{-1}$, $n+6f_s^{-1}$,..., $n+10f_s^{-1}$ are calculated and compared with the threshold.

- It can be observed that the channel weights are updated in Figure 8 for $n+5f_s^{-1}$ and $n+6f_s^{-1}$ instants. Because of this update, the channel state prediction that was free at $n+6f_s^{-1}$ in Figure 7 is changed to busy in Figure 8.

4. Performance evaluation

The performance of the proposed scheme is evaluated using 2 basic steps. In the first step, PRESCIENT is compared with 3 other channel access schemes. In the second step, the effect of configuration parameters on the performance of PRESCIENT is evaluated.

As mentioned in Section 1, microwave ovens and IEEE 802.11, IEEE 802.15.1, and other IEEE 802.15.4 devices are potential interferers in the 2.4 GHz ISM band. However, test results from [6] pointed out that microwave ovens have no serious negative effects on the 802.15.4-compliant devices if they are approximately 1 m away from the microwave oven. Similar to our preliminary test results, the literature [6,7] shows that the IEEE 802.15.1 and the IEEE 802.15.4 interferences have no remarkable effect on IEEE 802.15.4-compliant devices compared to IEEE 802.11 interference. Hence, in this section, all performance evaluations will be carried out under IEEE 802.11 interference since it is the most challenging for IEEE 802.15.4-compliant devices [6–9,13].

4.1. Comparison of PRESCIENT with the other schemes

In this subsection, packet loss rates of IEEE 802.15.4-compliant transceivers are employed to evaluate the performance of PRESCIENT. In the evaluations PRESCIENT will be compared with 3 other schemes: 1) IEEE 802.15.4 with static channel access, 2) IEEE 802.15.4 with random channel access, and 3) predictive channel access using the clustered RFSS [17]. PRESCIENT and the first two channel access schemes are implemented by using identical transceivers and their channel access performance are evaluated using the test bed described in Section 2. Because the predictive channel access using the clustered RFSS [17] scheme cannot be embedded in real IEEE 802.15.4-compliant hardware, CCA measurements of the test bed are logged and then the results are gathered by offline processing of the logs. During the tests, the nodes have to transmit 1 packet every 100 ms. In a static channel access scheme, the transmitter node accesses the channel and sends its packet every 100 ms. Random channel access schemes differ from the first scheme in terms of channel access decisions where the channel access is scheduled according to uniform distribution within 100 ms intervals. Finally, in PRESCIENT and predictive channel access using the clustered RFSS [17] (in short, Clustered RFSS), the channel access is scheduled to the instant with the lowest weight value. In Table 1, the performance of PRESCIENT gathered from Pair 1 and Pair 2 is compared with the other schemes in terms of free channel access performance where $f_s^{-1} = 10$ ms, $N = 1000$, $L = 120$, and $\lambda = -80$ dBm. We also run the test scenario by activating Pair 1 nodes only. The results observed are nearly the same as those presented in Table 1.

It is obvious that the proposed method is highly capable of detecting interference-free channel instants compared with the static and random channel access schemes. However, it should be kept in mind that there are instants where PRESCIENT predicts interference although the channel is free. This and similar issues affecting the performance of PRESCIENT will be evaluated in the next subsection.

Table 1. Comparative free channel access performance of the proposed method.

	Static channel access	Random channel access	Clustered RFSS [17]	PRESCIENT running on Pair 1	PRESCIENT running on Pair 2
# of successful transmissions	1851	1853	1936	1961	1962
# of packet losses	149	147	64	39	38
% of successful transmissions	92.55%	92.65%	96.8%	98.05%	98.10%
% of packet losses	7.45%	7.35%	3.2%	1.95%	1.90%

4.2. The analysis of the configuration parameters of PRESCIENT

In this subsection, the performance of PRESCIENT for varying configuration parameters is evaluated based on the percentage of false negative (FN) and false positive (FP) predictions. FP refers to the instants when the channel access is prevented although the channel is free. On the other hand, FN occurs at the instants when the channel access is allowed although the channel is busy. In this section, FN and FP rates are calculated for various scenarios by examining the impact of the following parameters:

- Channel activity monitoring module sample size, N;

- Prediction window sample size, L;

- Decision threshold, T_{THR};

- IEEE 802.11 traffic density.

In Figure 9, the performance of PRESCIENT is evaluated in terms of FP and FN rates of the channel access predictions for varying T_{THR} values where $N = 1000$, $L = 120$, $\lambda = -80$ dBm, and the IEEE 802.11 traffic load is approximately 0.074 E. Figure 9 shows the results for 1000 CCA samples. These results imply that the number of FPs is inversely proportional to T_{THR}. When T_{THR} increases, FP values decrease and FN values increase. Tests show that there is 75% to 97% decrease in the percentage of FN for T_{THR} values lower than 0.47. When we take the percentage of FPs into account, T_{THR} values between 0.2 and 0.47 are convenient for promising FN rates while causing 12% to 25% FPs.

We analyze the impact of traffic load on FN predictions in Figure 10. The y-axis shows the rate of reduction in the number of FNs due to the proposed scheme for different FP rates where $N = 1000$, $L = 120$, and $\lambda = -80$ dBm. Moreover, the rate of reduction in the number of FNs is calculated for 3 different IEEE 802.11 traffic traces, where Trace1, Trace2, and Trace3 have 0.022 E, 0.052 E, and 0.074 E IEEE 802.11 traffic loads, respectively. The results show that for the same FP rates, the proposed algorithm has slightly better FN rates for heavier IEEE 802.11 traffic loads, which is promising since channel access performance becomes more significant under heavier traffic.

FP and FN evaluations are further carried out for 0.074 E IEEE 802.11 traffic load for varying prediction window sample size (L) values where $T_{THR} = 0.33$, $N = 1000$, and $\lambda = -80$ dBm. The results given in Figure 11 show that the proposed scheme yields reasonable FN rates when L is greater than 90. However, since a high L value means making predictions over a longer window and consequently demanding more memory and processor allocation, it has to be adjusted carefully. Our tests show that L values between 90 and 180 are convenient for promising FN rates, taking memory usage and processor load into account.
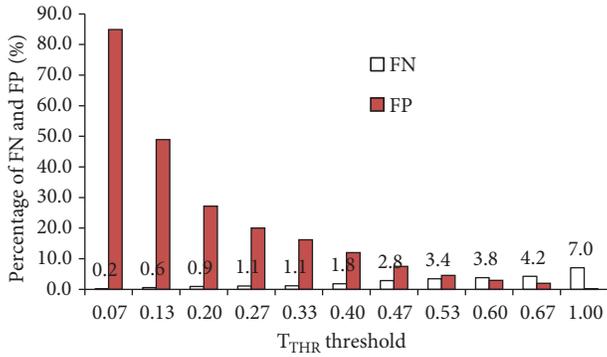
Figure 9. False negative and false positive percentages for varying T_{THR} under 0.074 E IEEE 802.11 traffic load.
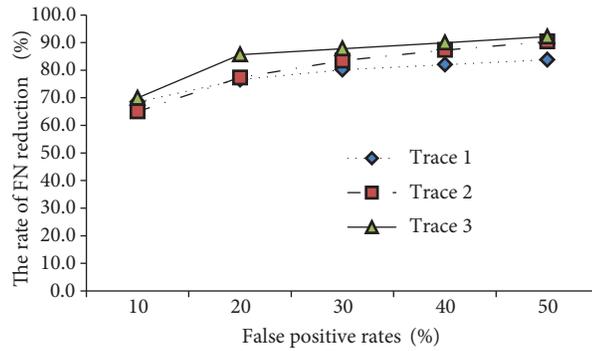

Figure 10. The rate of FN reduction for different FP rates under 3 different IEEE 802.11 traffic loads.

The impact of CAMM sample size (N) is examined in Figure 12. The FP and FN calculations are carried out for varying N values under 0.074 E IEEE 802.11 traffic load where $T_{THR} = 0.33$, $L = 120$, and $\lambda = -80$ dBm. In Figure 12, for all N values exceeding 2000, the proposed algorithm achieves slightly better FN and FP rates. Hence, we can state that CAMM sample size does not have a significant impact on the performance of the proposed scheme. This is one of the most important advantages of the proposed scheme since small N values require less processor allocation, which makes it feasible to embed the proposed algorithm into IEEE 802.15.4-compliant nodes. Figure 12 shows that N values between 400 and 800 are able to provide acceptable FN rates while requiring lower processing load than higher N values.
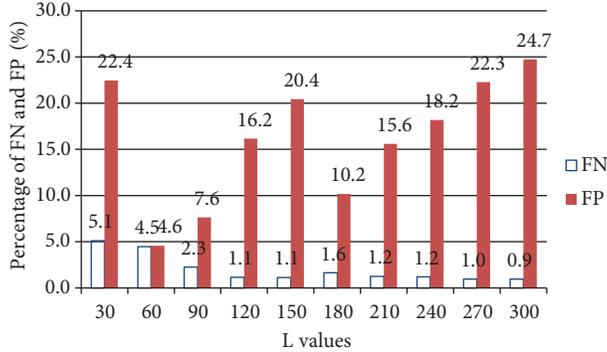

Figure 11. False negative and false positive percentages for varying prediction window sample sizes (L).
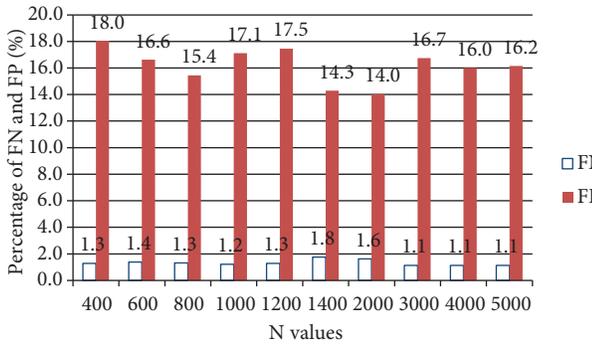

Figure 12. False negative and false positive percentages for varying CAMM sample sizes (N).

A channel access scheme for IEEE 802.15.4-compliant devices must be compact in terms of both code size and RAM usage. Therefore, during the implementation of PRESCIENT on test bed devices, code size and RAM usage should be optimized. The compiled code size and the RAM usage of PRESCIENT are given in Table 2.

Table 2 shows that both code size and RAM usage increase for larger prediction window sample sizes (L). On the other hand, CAMM sample size (N) has no effect on the amount of resource consumption. In summary, code size and RAM usage evaluations show that PRESCIENT is compact enough to be deployed on all types of resource-constrained IEEE 802.15.4-compliant devices.

Before concluding the performance evaluation section, we would like to discuss the latency and energy efficiency performance of PRESCIENT:

Table 2. A comparison of code size and RAM usage of PRESCIENT.

PRESCIENT configuration	Code size (bytes)	RAM usage (bytes)
PRESCIENT when N = 1000 and L = 60	756	80
PRESCIENT when N = 1000 and L = 120	816	140
PRESCIENT when N = 1000 and L = 180	876	200
PRESCIENT when N = 2000 and L = 60	756	80
PRESCIENT when N = 2000 and L = 120	816	140
PRESCIENT when N = 2000 and L = 180	876	200

- Latency: Since PRESCIENT is developed assuming that there exists interference in the channel, the worst case scenario considering latency is achieved under no coexisting traffic. In that condition, the IEEE 802.15.4-compliant device can access the channel whenever it wants. However, PRESCIENT will cause a hop-based delay because of the CCA measurement period, f_s^{-1}. The maximum and the mean values for this hop based delay are (f_s^{-1}) and $(f_s^{-1}/2)$, respectively. In our test bed conditions, these values occurred as 10 and 5 ms, respectively.

- Energy efficiency: PRESCIENT takes CCA measurements every f_s^{-1} s, which last for T_{CCA} seconds. Therefore, the main energy consumption caused by PRESCIENT becomes $E_{PRESCIENT}$:

$$E_{PRESCIENT} = f_s \times E_{CCA} \times T_{CCA}, \tag{7}$$

where E_{CCA} is the power consumption of the IEEE 802.15.4-compliant RF hardware during a CCA measurement. Hence, considering our IEEE 802.15.4-compliant test bed devices, $E_{PRESCIENT}$ becomes 0.454 mW/s, obtained as the result of $100 - 3546.10^{-2} \times 128.10^{-6}$

5. Conclusion

IEEE 802.11 devices have higher transmission power compared to IEEE 8022.15.4-compliant devices. As a consequence, coexistence has been one of the most significant challenges for IEEE 802.15.4-compliant devices because of their limited resources.

In this study, first the impact of the aggregated background IEEE 802.11 traffic on the 2.4 GHz ISM band was analyzed based on the CCA measurements of the IEEE 802.15.4-complaint nodes. Then a novel channel access scheme, called PRESCIENT (PREdictive channel access SCheme for IEee 802.15.4-compliaNT devices), was introduced. PRESCIENT predicts the instants of interference using previously measured RFSS samples. The performance of PRESCIENT was compared to 3 other channel access schemes. Then it was evaluated in terms of FP and FN channel access rates. The results show that PRESCIENT dramatically increases the free channel access performance of the IEEE-802.15.4-compliant devices under IEEE-802.11 traffic.

Since IEEE 802.11 is the strongest interferer for IEEE 802.15.4-compliant devices, currently we focus on the channel access performance of PRESCIENT under IEEE 802.11 interference. We think that our work provides first-step analysis to employ prediction for channel access under interference.

Furthermore, we plan to examine the effect of important IEEE 802.15.4 parameters, inner-network interference, and multihop routing as future work. We also plan to combine PRESCIENT with a dynamic channel selection mechanism in order to improve performance.

References

[1] IEEE. IEEE 802.15.4b Standard, Wireless Medium Access Control and Physical Layer Specification for Low Rate Wireless Personal Area Networks. New York, NY, USA: IEEE, 2006.

[2] IEEE. IEEE Standard 802.11–2007, IEEE Standard for Information Technology - Telecommunications and Information Exchange between Systems - Local and Metropolitan Area Networks - Specific Requirements - Part 11: Wireless LAN Medium Access Control (MAC) and Physical Layer (PHY) Specifications. New York, NY, USA: IEEE, 2007.

[3] IEEE. IEEE Standard 802.15.1-2005, IEEE Standard for Information Technology - Telecommunications and Information Exchange between Systems – Local and Metropolitan Area Networks - Specific Requirements - Part 15.1: Wireless Medium Access Control (MAC) and Physical Layer (PHY) Specifications for Wireless Personal Area Networks (WPANS). New York, NY, USA: IEEE, 2005.

[4] Rondeau TW, D'Souza MF, Sweeney DG. Residential microwave oven interference on bluetooth data performance. IEEE T Consum Electr 2004; 50: 856–863.

[5] Kushiro N, Katsukura M, Nakata M, Higuma T, Ito Y. Performance of ad-hoc wireless network on 2.4 GHz band in real fields. IEEE T Consum Electr 2008; 54: 80–86.

[6] Sikora A, Gora VF. Coexistence of IEEE 802.15.4 with other systems in the 2.4GHz ISM band. In: IEEE 2005 Instrumentation and Measurement Technology Conference; 17–19 May 2005; Ottawa, Canada. New York, NY, USA: IEEE. pp. 1786–1891.

[7] Shin SY, Park HS, Choi S, Kwon WH. Packet error rate analysis of ZigBee under WLAN and Bluetooth interferences. IEEE T Wirel Commun 2007; 6: 2825–2830.

[8] Petrova M, Riihijarvi J, Mahonen P, Labella S. Performance study of IEEE 802.15.4 using measurements and simulations. In: IEEE 2006 Wireless Communications and Networking Conference (WCNC); 3–6 April 2006; Las Vegas, NV, USA. New York, NY, USA: IEEE. pp. 487–492.

[9] Pollin S, Ergen M, Dejonghe A, Van der Perre L, Catthoor F, Moerman I, Bahai A. Distributed cognitive coexistence of 802.15.4 with 802.11. In: IEEE 2006 CrownCom; 8–10 June 2006; Mykonos, Greece. New York, NY, USA: IEEE. pp. 1–5.

[10] Shuaib K, Boulmal M, Sallabi F, Lakas A. Co-existence of ZigBee and WLAN - a performance study. In: 2006 Wireless Telecommunications Symposium (WTS); 27–29 April 2006; Los Angeles, CA, USA. New York, NY, USA: IEEE. pp. 1–5.

[11] Angrisani L, Bertocco M, Fortin D, Sona A. Experimental study of coexistence issues between IEEE 802.11b and IEEE 802.15.4 wireless networks. IEEE T Instrum Meas 2008; 57: 1514–1523.

[12] IEEE P802.15 Working Group for Wireless Personal Area Networks (WPANs). Coexistence Analysis of IEEE Std 802.15.4 with Other IEEE Standards and Proposed Standards. White Paper. New York, NY, USA: IEEE, 2010.

[13] Yang D, Xu Y, Gidlund M. Wireless coexistence between IEEE 802.11- and IEEE 802.15.4-based networks: a survey. Int J Distrib Sens N 2011; 2011: 912152.

[14] Torabi N, Wong WK, Leung VCM. A robust coexistence scheme for IEEE 802.15.4 wireless personal area networks. In: IEEE 2011 Consumer Communications and Networking Conference (CCNC); 9–12 January 2011; Las Vegas, NV, USA. New York, NY, USA: IEEE. pp. 1031–1035.

[15] Kang MS, Chong JW, Hyun H, Kim SM, Jung BH, Sung DK. Adaptive interference-aware multi-channel clustering algorithm in a ZigBee network in the presence of WLAN interference. In: 2007 2nd International Symposium on Wireless Pervasive Computing; 5–7 February 2007; San Juan, Puerto Rico. New York, NY, USA: IEEE. pp. 200–205.

[16] Mahalin NH, Sharifah HS, Yusof SKS, Fisal N, Rashid RA. RSSI measurements for enabling IEEE 802.15.4 coexistence with IEEE 802.11b/g. In: IEEE 2009 TENCON; 23–26 January 2009; Singapore. New York, NY, USA: IEEE. pp 1–4.

[17] Coplu T, Oktug S. Predictive channel access scheme for wireless sensor networks using received signal strength statistics. In: IEEE 2011 Consumer Communications and Networking Conference; 9–12 January 2011; Las Vegas, NV, USA. New York, NY, USA: IEEE. pp. 590–594.

[18] Pollin S, Ergen M, Ergen SC, Bougard B, Van der Perre L, Moerman I, Bahai A, Varaiya P, Catthoor F. Performance analysis of slotted carrier sense IEEE 802.15.4 medium access layer. IEEE T Wirel Commun 2008; 7: 3359–3371.

[19] Lal D, Maneshwar A, Herrmann F, Uysal-Biyikoglu E, Keshavarzian A. Measurement and characterization of link quality metrics in energy constrained wireless sensor networks. In: IEEE GLOBECOM; 1–5 December 2003; San Francisco, CA, USA. New York, NY, USA: IEEE. pp. 446–452.

[20] Srinivasan K, Levis P. RSSI is under appreciated. In: 2006 Third Workshop on Embedded Networked Sensors (EmNets); 30–31 May 2006; Cambridge, MA, USA.